Application of the fluorescent fingerprinting strategy for the verification of electron-beam and X-ray irradiation of potato tubers

Anna V. Shik
M.V.Lomonosov Moscow State University
Evgenii V. Skorobogatov
M.V.Lomonosov Moscow State University
Ulyana A. Bliznyuk
M.V.Lomonosov Moscow State University
Alexander P. Chernyaev
M.V.Lomonosov Moscow State University
Valentina M. Avdyukhina
M.V.Lomonosov Moscow State University
Polina Yu. Borschegovskaya
M.V.Lomonosov Moscow State University
Sergey A. Zolotov
M.V.Lomonosov Moscow State University
Maksim O. Baytler
M.V.Lomonosov Moscow State University
Irina A. Doroshenko
M.V.Lomonosov Moscow State University
Tatyana A. Podrugina
M.V.Lomonosov Moscow State University
Mikhail K. Beklemishev (beklem@inbox.ru)
M.V.Lomonosov Moscow State University

Article

Keywords:

Posted Date: June 21st, 2022

DOI: https://doi.org/10.21203/rs.3.rs-1739042/v1

Abstract

High-energy electron beam and X-ray processing of foods can be used for the sterilization purposes, and the treatment of seed potatoes can reduce its field damage by pests and diseases. Chromatography–mass-spectrometry methods demonstrated notable changes in the chemical composition of treated foods, but it is not an affordable technique. This paper is aimed at developing more simple methods for revealing the fact of radiation treatment of potato tubers and approximate dose detection. We used a “fingerprinting” strategy that does not involve the determination of the amount of any particular chemical compound; instead, the effect of the potato extracts on the rate of indicator reactions with the participation of carbocyanine dyes is measured: one type of reaction is catalytic oxidation of the dye and the other involves an aggregational process. The dye content was followed by its near-IR fluorescence intensity and visible light absorption. The potatoes not subjected to treatment or irradiated with different doses (10, 100, 1,000 and 10,000 Gray) yielded different signals and eventually different patterns in the score plots of principal component and discriminant analysis. Non-irradiated tubers can be confidently distinguished from those irradiated with a high dose, and the order of the dose received can be estimated with 89–100% accuracy.

Introduction

Radiation treatment in food industry has been studied for several decades. Irradiation not only extends the shelf life of foods, keeping bacteria to a minimum, but it can also ensure proper phytosanitary conditions of seedstock. Gamma irradiation generated by ^{60}Co and ^{137}Cs isotopes, electron beams with the energy up to 10 MeV and bremsstrahlung radiation with the energy up to 5 MeV generated by electron accelerators are allowed as sources for food irradiation[1]. Researchers suggest using X-ray irradiation with the energy up to 200 keV generated by X-ray tube for surface treatment of fruit and vegetable which allows surface layers of a product to absorb a higher dose than the inside layers[2].

Despite the benefits of food radiation treatment, such as high efficiency and low cost, the absence of chemical traces and post thermal effects, irradiation may compromise the taste, color, and smell of treated foods. All these negative effects result from the formation of free radicals during irradiation, which are highly reactive and eventually form lipid hydroperoxides. These reactive substances invoke a number of chemical reactions entailing metabolic disorder, as well as destruction of enzymes, intracellular structures, and DNA, which leads to substantial changes in chemical composition of foods[3,4]. The regulations concerning food irradiation vary from country to country[5].

The dose absorbed by the foods is usually measured by chemical dosimerty, a group of well-developed techniques that employs UV-visible and fluorescence methods for the determination of doses[6,7]. However, a dosimeter must be irradiated along with the food sample to determine the dose.

Post-irradiation dose determination methods were developed by using electron spin resonance spectrometry (ESR). This technique is developed for foods containing bones[8], shells[9] or seeds[10] and

requires the use of ESR instruments.

The chemical changes in the samples invoked by irradiation can be detected by using purely chemical methods. Lipid peroxides, a product of radiation treatment, can be determined by Kreis test that is based on the reaction of peroxides with phloroglucinol and colorimetric detection of the reaction product[11]. Spectrophotometric method, applied to determine malondialdehyde and the products of peroxides decomposition in foods, is based on the reaction with 2thiobarbituric acid[12]. These methods cannot determine the doses used in food treatment due to their limited sensitivity.

Changes in the concentrations of many volatile compounds in irradiated food samples containing fats can be determined using gas chromatography – mass-spectrometry technique (GC-MS). Decomposition of fatty acids decreases the concentration of alcohols, aldehydes, ketones and other organic compounds, which can be markers for chemical changes leading to taste, color, and smell deterioration[13,14]. GC–MS is a sophisticated technique that requires expensive instrumentation and skilled personnel.

In this paper we consider fingerprinting techniques: a group of methods for distinguishing samples of similar composition, relying on obtaining spectral or other information from the sample with its subsequent analysis by pattern recognition (chemometrics) techniques, without identification of individual components. Fingerprinting techniques can establish the difference between samples, but not their chemical composition. These features make fingerprinting techniques rapid, inexpensive and versatile.

Fingerprinting techniques have been used in solving various practical tasks: revealing the adulterations of foods[15] and dietary supplements[16], determining the manufacturer[17,18], discriminating the sorts of oils[19], alcoholic beverages[20] and soils[21], determining gender by a dactylogram[22] and identifying patients with malignancies[23]. Many fingerprinting methods rely on fluorescence spectral data. In most cases, intrinsic fluorescence of the samples is employed[24,25].

A less popular but more efficient fingerprinting technique involves the addition of fluorophores to samples. In this strategy, not only fluorescent compounds contribute to the signal but also the compounds which can interact with the added fluorophore and thus affect its quantum yield[26–32]. This approach allows for identification of counterfeit drugs[26], discrimination of phosphates[27] and various mixtures of drugs[28,29].

The purpose of this research was to develop a chemical fingerprinting method for distinguishing irradiated potato tubers treated by accelerated electrons and X-rays from non-irradiated ones, and if possible, classify the tubers irradiated with different doses.

Materials And Methods

Materials. Potatoes of two different varieties were purchased locally. Chemical reagents used in the research were obtained from Sigma–Aldrich. The carbocyanine dyes (Fig. 1) were synthesized by the authors following the published protocols: dye **1**[33], dye **2**[34], dye **3**[35], dye **4**[36].

Experimental techniques

Electron beam treatment. Potato tubers were subjected to radiation treatment as single pieces. The irradiation was carried out at Skobeltsyn Institute of Nuclear Physics (Moscow, Russia) using continuous wave linear electron accelerator UELR-1-25-T-001 with an energy of 1 MeV and a maximum average beam power of 25 kW. The beam current varied from 50 to 500 nA and the ambient temperature was about 20°C. The tubers were placed on a 35 mm × 182 mm duralumin plate which was located 12.5 cm from beam input and irradiated with 10 Gy, 100 Gy, 1 kGy and 10 kGy from two sides. In one experiment each dose was applied to 6 tubers, and 6 tubers were left as controls. The absorbed dose was estimated taking into account the charge absorbed by duralumin plate. The algorithm for dose estimation is described in paper [37].

X-ray irradiation treatment. Two-side X-ray irradiation of potatoes was performed at the Physics Department of Moscow State University using DRON UM-2 unit with power supply PUR5/50 and X-ray tube BSV-23 with a copper anode. Prior to irradiation the tubers were cut into 6 mm thick, 6 mm long and 15 mm high parallelepipeds which were then placed in 2-mL polypropylene tubes with the diameter of 9 mm. The sample was placed directly in front of the beryllium window of the X-ray tube. The tube current was 26 mA and the voltage was 30 kV. The irradiation was carried out in the room with the ambient temperature of 20 ºC. The samples were irradiated with 100 Gy, 1 kGy and 5 kGy doses. Each dose was applied to two identical samples; two non-irradiated samples were left as controls. The doses absorbed by the samples were estimated as described[37].

Dose distribution in potato samples. For the sphere, computer simulation based on Monte-Carlo method, with the toolkit GEANT4, was performed for bilateral irradiation of spherical water phantom with the diameter of 4 cm and the density of 1 g/cm^3 which imitated a potato tuber. The phantom was irradiated with 10^6 electrons having the energy of 1 MeV. The electron source was a 5 cm square located 2.5 cm away from the phantom.

A cube with the edge of 4 cm, split into 20 × 20 × 20 cube cells having the edge of 2 mm, with the same center as the spherical water phantom was irradiated to estimate the dose distribution throughout the entire volume of the phantom (Fig. 2,a). For the sphere the simulation only took into account the cells which were fully filled with water.

In the simulation a 6 mm thick, 6 mm long and 15 mm high water parallelepiped was irradiated with 10^8 photons as shown in Fig. 2,b. The photon spectrum peaked at 9 keV which corresponds to characteristic radiation of copper, while the bremsstrahlung spectrum reached 26 keV[13].

The water parallelepiped was divided into 60 × 60 × 150 cube cells having the edge of 0.1 mm.

Sample preprocessing. After irradiation with electrons, the potato tubers were skinned using a vegetable peeler. A 1 mm thick layer from the parts of the samples which had the maximum exposure to electrons and X-rays were then peeled off; the 4 g portions of the shreds were placed in 20-mL polypropylene vials, and 10 mL of water purified using a Millipore water purification unit were added to the mixture. To avoid oxidation of the extracts with atmospheric oxygen, which leads to their coloration, 100 μL of 0.1 mol/L solutions of ascorbic acid or sodium sulfite were added as antioxidants.

After irradiation with X-rays, 1 mL of deionized water and 15 μL of 0.1 mol/L ascorbic acid solution were added to each sample in the plastic test-tube.

The samples were then placed on an orbital shaker for 9 h followed by the subsequent storage during 10–12 h before analysis.

Indicator reactions using carbocyanine dyes. The aqueous extracts of potatoes were introduced into oxidation-reduction (redox) and aggregation-type indicator reactions. For the redox reactions, the following solutions were pipetted to the 96-well polystyrene plates (Thermo Scientific Nunc F96 MicroWell, white, cat. No 136101) in the indicated order: 1) phosphate buffer (pH 7.4, 0.067 mol/L), 30 μL; 2) water (up to a total volume of 300 μL); 3) 1 mmol/L cetyltrimethylammonium bromide (CTAB), 30 μL; 4) potato aqueous extract, 25 μL; 5) 1 mol/L H_2O_2, 30 μL, 6) 1 mmol/L $CuSO_4$, 30 μL; 7) 0.1 g/L dye in water, 30 μL. Multichannel pipettes were used to fill a large number of wells. The moment of dye addition was taken as the start of the reaction.

For the aggregation-type reaction, the following solutions were mixed in the plate: 1) buffer (pH 7.4) or HCl solution (0.1 mol/L, for dye **1**), 30 μL; 2) water (up to a volume of 300 μl); 3) CTAB 1 mmol/L, 70 μL (for dye **1**) or sodium *n*-dodecyl sulfate (SDS), 8 mmol/L (dye **4**), 30 μL; 4) potato extract, 25 μL; 5) dye, 0.1 g/L (dye **4**) or 0.04 g/L (dye **1**) in water, 30 μL.

In one set of experiments, the potato extract was introduced in one aggregation-type indicator reaction (with dye **1** or **4**) and two redox-type reactions (with dyes **1**, **2** or **3**). The reactions of the potato extracts with added ascorbic acid and sulfite as antioxidants were conducted separately. The visible and NIR fluorescence images of the 96-well plates with the reaction system were taken every few minutes for the redox reactions (during 15–30 min) and once for the aggregation-type reaction. The photographs in visible light were taken by a smartphone camera; near-IR fluorescence was monitored using a home-made NIR visualizer including red LEDs (660 nm) as light source and a Nikon D80 photo camera with a light filter cutting off the visible light up to 700 nm[33]. For each radiation dose and control (non-irradiated samples), 1–3 potato tubers were studied, and 5 parallel runs were performed for each tuber (5 wells of the plate were filled).

Data treatment. The images were digitized using ImageJ software (Fiji) to obtain the mean intensities corresponding to separate wells. No RGB splitting was performed, as no wavelength maxima differed

between samples. The results of digitization of the photographic images were presented as data tables with columns corresponding to different indicator reactions and various reaction times; the maximum number of columns was 22. The rows of the data table corresponded to different runs (5 parallel runs for each tuber, 2 or 3 tubers for each dose, 4–5 doses including the zero dose), so that the maximum number of rows was 75. An example of data table is shown as Supplementary Table S1.

The data were subjected to principal component analysis (PCA) using the Unscrambler X (Camo Software, Norway) or linear discriminant analysis (LDA) using the XLSTAT Excel (Addinsoft, USA) add-on. The results were visualized in the form of scores plots in the coordinates of principal components PC1–PC2 and PC1–PC3 or LDA factors F1–F2 and F1–F3. Mahalanobis distances (MD)[38] between the validation points and groups of points corresponding to certain doses were used in estimating the accuracy of discrimination. Ellipses in the plots were constructed arbitrarily, as a guide to the eye.

Results And Discussion

Dose distribution over the sample. The simulation estimated the dose absorbed by each cell and standard deviation to assess absorbed dose error:

$$D_i = \frac{\sum_{j=1}^{N_i} E_{ij}}{m_i}$$

1

where $\sum_{j=1}^{N_i} E_{ij}$ is the sum of energies lost in *i* cell, N_i is the number of events in i cell, and m_i is the mass of i cell.

$$S_i = \sqrt{(\frac{1}{N_i - 1}\sum_{j=1}^{N_i} E_{ij}^2 - \left(\frac{1}{N_i - 1}\sum_{j=1}^{N_i} E_{ij}\right)^2)}$$

2

where $\sum_{j=1}^{N_i} E_{ij}^2$ is the sum of E_j^2 values in *i* cell. The dose in each cell was divided by the maximum dose value recorded in the water sphere and water parallelepiped. The relative dose value in each cell was color-coded to show the dose distribution in the phantoms (Fig. 3a, b).

The sides A and B of water sphere hit by 1 MeV electrons from the opposite directions got the maximum dose to compare with the sides C and D (Fig. 3a). In view of such a dose distribution, a 3–4 mm thick layer of water sphere from sides A and B were irradiated with 1 MeV electrons. According to that, a 1-mm thick skin was removed from the tubers, and a 1-mm thick layer of the tuber was peeled for the subsequent extraction.

In water parallelepiped, the layers located close to beryllium window of the X-ray tube received the maximum dose (Fig. 3b). Further, the dose plummeted as photons were penetrating deeper than 1 mm into the phantom.

Development of a chemical test. The task was to differentiate between potato tubers irradiated with different doses and the non-irradiated samples. Our attempt to use the classical fingerprinting approach for this purpose was not successful: the samples did exhibit intrinsic fluorescence, but its intensity did not change as a result of irradiation. The technique of adding fluorophores to potato samples was not successful either: the signal of the added dye did not change with the dose.

We had to turn to a more sophisticated fluorescent fingerprinting technique which we suggested recently. This strategy relies on the effect of analytes on two types of indicator reactions: (1) catalytic oxidation of a dye with H_2O_2[39] and (2) the formation of fluorescent aggregates of the dye with the analyte and a surfactant[33,40]. By the analytes we imply reactive chemical components of the sample whose concentration could have changed as a result of radiation treatment. In system (1), the analytes are supposed to bind with the transition metal ion (Cu^{2+} or Pd^{2+}) that catalyzes the oxidation of a carbocyanine dye with hydrogen peroxide. As a consequence, the oxidation reaction rate changes, which is tracked by the visible light absorption and by the fluorescence intensity change of the carbocyanine dye in solution[39].

In system (2), the reactive analytes form a “hydrophobic ion pair”[40] with an oppositely charged surfactant. For the biological species supposedly containing in the sample, which are for the most part anionic, a cationic surfactant cetyltrimethylammonium bromide (CTAB) was used. The hydrophobic ion pairs were found[33] to incorporate hydrophobic dyes, which is accompanied by fluorescence enhancement. The types (1) and (2) indicator reactions were studied by us earlier, and the concentration conditions for the present research were selected based on the previous studies[35,39]. In reactions of type (2) we employed hydrophobic dyes prone to forming fluorescent aggregates with a surfactant and an oppositely charged analyte (dyes **1** and **4**)[33,35,39]. In type (1) reactions we used less hydrophobic and more water-soluble carbocyanines that could be easily oxidized by H_2O_2 (dyes **2–4**)[35,39]. The concentrations of the oxidant and metal ion-catalyst were chosen to provide a reaction rate convenient for observation (1 M hydrogen peroxide, 1 mM Cu^{2+}). The general strategy is schemed in Fig. 4.

The development of signal over time was recorded photographically in the visible and near-IR region (Fig. 5, each three adjacent columns represent a sample). It can be seen that the differences between samples are not very pronounced. There was a question, whether these differences were sufficient to distinguish between the absorbed doses. To solve this problem, the images were digitized and subjected to chemometric treatment. The indicator reactions and concrete images used in chemometric treatment are listed in Supplementary Table S2. The results were presented as scores plots allowing to more explicitly visualize of the differences between the samples.

Discrimination of tubers irradiated by an electron beam. For the set of experiments No 1, the different doses were not discriminated by using principal component analysis (PCA). We turned to discriminant analysis (LDA), which is a supervised technique, i.e. the software is informed about which signals belong to which class (irradiation dose). Before performing the LDA procedure, all data were divided into training set and validation set. The training set is used by the LDA software to establish the relationship between the sample and its dose (create the model), and the validation set is used to verify the quality of this model. As a compromise, we chose a validation set size as 28–30% of all data (14–15 samples out of the total amount of 50). A larger number of validation samples would shorten the training set and impede the discrimination quality.

LDA yields a 4-dimensional score plot in the coordinates of factors F1–F4. The potato samples irradiated with different doses are represented as groups of points in this plot. The accuracy of discrimination by LDA technique is estimated as the percentage of correctly assigned validation samples. For example, the points in Fig. 6 correspond to 36 training and 14 validation samples. Since the discrimination is not perfect, it is difficult to assign some of the validation points to specific groups of training samples. The software considered such assignment as correct if the Mahalanobis distance between the validation point and the training sample group of the correct dose was minimal among the distances to the other groups. In other words, the correctly assigned validation point should be located closer to the group of points of the dose it originated from. The distances for such disputed points are illustrated in Fig. 6. Accuracy was calculated as the ratio of the number of correctly assigned validation points to the total number of validation points; the software presented this result as confusion tables (Table 1).

Overall, for the data demonstrated in Fig. 6, the tubers irradiated with an unknown dose can be assigned to one of the doses (10; 100; 1,000 and 10,000 Gy) with 100% accuracy using the basic data set.

Table 1
An example of confusion matrix for the validation points obtained by the XLSTAT software. Incorrectly predicted doses are shown in bold font

True dose, Gy	Predicted dose, Gy					Total No of points	Accuracy*
	0	10	100	1,000	10,000		
0	1	0	**1**	0	0	2	50,0%
10	0	3	0	0	0	3	100,0%
100	0	0	3	0	0	3	100,0%
1,000	0	0	0	2	**1**	3	66,7%
10,000	0	0	0	0	3	3	100,0%
Total No of points	1	3	4	2	4	14	**85,7%**

* Number of accurately predicted values / total number of validation points.

The red arcs in graph (*a*) connect the validation points and the barycentres of the nearby groups corresponding to certain absorbed doses shown as black squares; the Mahalanobis distances in the space of factors F1–F4 are shown in red numbers beside the arcs. Validation procedure can be considered, for example, for a validation point located between the doses of 10 kGy and 100 Gy; this point is seemingly closer to the 10 kGy group; however, in the other dimension (F1–F3) that point is at a greater distance from the 10 kGy group. Quantitatively, the 4D distances from this point to 10 kGy and 100 Gy groups are 8.9 and 6.1 units, respectively (shown by the red arcs), which implies that the point belongs to the 100 Gy group. Similar situations can be viewed for the other validation points.

Table 2
Accuracy of discrimination of potato tubers irradiated with electron beam for various data sets of experiment No 1

Data set used for treatment	Number of data columns*	Accuracy, %**
Basic data set	22	100
Aggregation reaction of dye **1** removed	20	78
Oxidation reaction of dye **3** removed	16	78
Oxidation reaction of dye **2** removed (samples with sulfite)	16	86
Oxidation reaction of dye **2** removed (samples with ascorbate)	14	86
Only dye **2** reactions are used	12	86
Only NIR images are used	12	80
Columns with the highest standard deviations are used***	7	64
Data are selected by the largest visual difference between photographs	5	57
* Each column contains data for one indicator reaction at a certain reaction time (concrete characteristics of the data cloumns are given in Supplementary Table S2).		
** Percentage of validation points correctly assigned to their groups (automatically calculated based on the comparison of Mahalanobis distances to the groups. The results were presented as tables similar to Table 1).		
*** Standard deviations were calculated for the columns as measures of data diversity between samples.		

Reduction of data. Discrimination of potatoes irradiated with different doses was based on 3–4 indicator reactions. In order to reduce the number of experiments, an attempt was made to find out whether it was possible to reduce the amount of data. If an indicator reaction (based on dyes **1**, **2** or **3**) was excluded from the basic data set of 22 columns to give a reduced set of 14–20 columns, the discrimination accuracy dropped to 78–85% (Table 2). The same accuracy was observed if only dye **2** reaction was

used or only near IR images were treated (12 columns). Further reduction of data resulted in substantial deterioration of accuracy. The corresponding score plots are given in Supplementary Fig. S1, a–f.

Effect of potato variety. Experiment No 1 was conducted with the potatoes of one variety. However, a situation may arise where the tubers irradiated with known doses belong to one variety, while the tubers irradiated with an unknown dose are of a different variety. For this reason, in experiment No 2 we studied two different potato varieties (X and Y), three tubers of each. The indicator reactions used in experiment No 2 were the same as those in experiment No 1. The dose of 10 Gy was not used in experiment No 2 in order to reduce the number of rows in the data table.

When only the samples of variety X were considered, 100% accurate discrimination of the samples according to the doses was achieved (Fig. 7,a). For variety Y, the 100 Gy and 1,000 Gy samples were poorly separated (Fig. 7,b). Due to that, all doses were correctly assigned only in 93% cases (the average of 5 validation runs, each run was performed with 48 training and 12 random validation samples). For both varieties it was possible to confidently distinguish between the irradiated and non-irradiated samples.

When all data were treated without the distinction of X and Y varieties, the groups of points were also partly overlapping (Fig. 7,*c*). The accuracy of determination of the dose for the combined varieties was 89% (the result of validation procedure repeated 5 times with 25 validation and 95 training samples). Consequently, the discrimination of doses can be achieved even for the tubers of different varieties, though it can be less efficient that within one variety.

Discrimination of tubers irradiated by X-rays. The same dose of electron beam radiation can be more efficient than X-rays since it can destroy microorganisms more efficiently, as it was found in the study of irradiation of turkey meat[13]. Nevertheless, we explored the feasibility of discriminating between the X-ray doses absorbed by the potato samples. Two tubers of one variety were studied. Technically, the whole tubers could not be treated, for which reason the potato pieces sized 6 mm × 6 mm × 15 mm were placed in the Eppendorf tubes and irradiated during 50 s to 21 min, which corresponded to doses of 0, 100, 1000, and 5000 Gy. After irradiation, the samples were extracted with water similarly to the samples irradiated with an electron beam, and after 24 h of extraction, the same indicator reactions were carried out in the 96-well plate. Each sample was measured in 5 parallels, which gave totally 40 samples (2 tubers × 4 doses × 5 parallels). The data were collected 3 times during 20 min for the redox reaction, which totally yielded 24 data columns. The whole data set was used for the discriminant analysis treatment.

The results shown in Fig. 7,d demonstrate that the X-ray doses can be completely discriminated. Validation was performed 5 times with a random validation set (each time with 32 training and 8 validation samples). Out of the total number of 40 validation samples, 38 were assigned correctly, which corresponds to the discrimination accuracy of 95%.

Advantages, limitations and prospects. A limitation of the suggested chemical fingerprinting method is the necessity to analyze the reference samples of known composition along with the unknown ones. In

other words, the samples irradiated with known doses and control samples should be treated simultaneously with the unknowns. Theoretically, the measurements of known samples could be performed in advance, but the real day-to-day reproducibility of the optical signal in the indicator reactions is not perfect, and the results obtained on one day cannot be reliably used on another day. This is a consequence of the nature of the reactions used in this method and a price to pay for their sensitivity.

In this study, we extracted the samples on the day of irradiation. Some additional research effort is needed to find out how long after exposure it is still possible to determine the dose (for example, if the sample was irradiated a week or two ago).

It is clear that the properties of potato samples may strongly depend on the variety, conditions of growth and other factors, which can eventually alter the discrimination efficiency. This work only shows the fundamental possibility of determining the order of the absorbed dose. Other foods should be also studied in this regard.

The fingerprinting technique does not allow us to reveal the nature of compounds formed in the irradiated samples that influence the indicator reaction rate and allow for the discrimination of samples. However, this knowledge is unnecessary for solving practical tasks.

The advantage of this method over chromatography techniques is its relative simplicity with no spectral or other sophisticated instrumentation involved except for the photo cameras and red light LED source. In this study we used synthesized carbocyanines but the protocol can be later adapted to commercially available dyes. The accuracy of discrimination can be further improved by implementing new indicator reactions that would be more sensitive to the composition of irradiated samples.

Conclusion

The suggested chemical test is capable of discriminating the doses absorbed by potato samples irradiated with X-rays or an electron beam. Differently irradiated samples demonstrate different indicator reaction rates due to the formation of reactive chemical compounds as a result of treatment. The non-irradiated tubers can be distinguished from the tubers irradiated with low doses (100 Gy and, in some experiments, 10 Gy) by using discriminant analysis technique. Estimation of the absorbed doses differing by an order of magnitude is also possible: the accuracy of discrimination between such doses is 89% (for a mixture of two different potato varieties). The suggested strategy can be potentially applied to other types of foods.

Declarations

Data availability. Original data is available as MS Excel files or photographic images from M.K.B. upon request.

Acknowledgments

The authors thank Dr. Andrey V. Garmash for providing his software for the calculation of Mahalanobis distances.

Funding

This research was supported by the Russian Science Foundation (grant No 20-13-00330).

Author contributions

A.V.S, E.V.S. and M.O.B. performed the chemical testing; A.P.C., V.M.A., P.Yu.B. and S.A.Z. was the radiation treatment team. I.A.D. and T.A.P. was the chemical synthesis team. M.K.B. and U.A.B. wrote the manuscript text, they were the joint supervisors for the whole work. E.V.S. prepared graphs 6–7. M.K.B. provided funding for the analytical chemistry part of work and supervised it, U.A.B. supervised the physical aspect of work and provided the article process charge, T.A.P. supervised the synthetic part of work.

Competing interests

The authors declare no competing interests.

Additional information

Correspondence should be addressed to M.K.B.

References

1. ISO 14470:2011. Food irradiation – Requirements for the development, validation and routine control of the process of irradiation using ionizing radiation for the treatment of food.
2. Prakash, A., Omelas-Paz, J. Irradiation of fruits and vegetables. Chapter 17 in book: Postharvest technology of perishable horticultural commodities. P. 563–589. https://doi.org/10.1016/B978-0-12-813276-0.00017-1 (2019).
3. Riley, P. A. Free Radicals in Biology: Oxidative Stress and the Effects of Ionizing Radiation. Int. J. Radiat. Biol. **65**, 27–33. https://doi.org/10.1080/09553009414550041 (1994).
4. Dokuchaeva, I.S., Gumerova, G.Kh. & Khakimova, E.G. Problems of the technology of radiation sterilization of food products. Bull. Kazan Technol. University **19**, 169–171. https://cyberleninka.ru/article/n/problemy-tehnologii-luchevoy-sterilizatsii-pischevyh-produktov (2016).
5. Commission staff working document evaluation of the EU legal framework on food irradiation (Directives 1999/2/EC and 1999/3/EC) https://eur-lex.europa.eu/legal-content/EN/TXT/HTML/?uri=CELEX%3A52021SC0225.
6. Ergun, E.A. New Fluorometric Dosimetry for Low-medium Gamma Radiation Doses. J. Fluoresc. **31**, 941–950. https://doi.org/10.1007/s10895-021-02715-2 (2021).

7. Lu, H., Xie, J., Wang, X.Y. *et al.* Visible colorimetric dosimetry of UV and ionizing radiations by a dual-module photochromic nanocluster. Nat. Commun. **12**, 2798. https://doi.org/10.1038/s41467-021-23190-0 (2021).
8. Desrosiers, M.F. Electron Spin Resonance for Monitoring Radiation-Processed Meats Containing Bone. Food Sci. **56**, 1104–1105 https://doi.org/10.1111/j.1365-2621.1991.tb14653.x (1991).
9. Desrosiers, M.F., Le, F.G., Harewood, P.M., Josephson E.S. & Montesalvo, M. Estimation of the Absorbed Dose in Radiation-Processed Food. 4. EPR Measurements on Eggshell. J. Agric. Food Chem., 41, 1471–1475 (1993).
10. Sezer, M.Ö., Kaplan, N. & Sayin, U. ESR analysis of natural and gamma irradiated coriander (*Coriandrum sativum L.*) seeds. Radiation Effects and Defects in Solids, **172**, 815–823 https://doi.org/815-823 10.1080/10420150.2017.1402329 (2017).
11. Vaghela, K.D., Chaudhary, B.N., Mehta, B.M. *et al.* Comparative appraisal of Kreis methods for the assessment of incipient rancidity in ghee. Brit. Food J. **120**, 240–250. https://doi.org/10.1108/BFJ-04-2017-0235 (2018).
12. Zeb, A. & Ullah, F. A simple spectrophotometric method for the determination of thiobarbituric acid reactive substances (TBARS) in fried fast foods. J. Analyt. Meth. Chem., No 1, 9412767. https://doi.org/10.1155/2016/9412767 (2016).
13. Bliznyuk, U., Avdyukhina, V., Borshchegovskaya, P. *et al.* Effect of electron and X-ray irradiation on microbiological and chemical parameters of chilled turkey. Sci. Rep. **12**, 750– https://doi.org/10.1038/s41598-021-04733-3 (2022).
14. Bliznyuk, U.A., Avdyukhina, V.M., Borshchegovskaya, P.Yu, Bolotnik, T.A., Ipatova, V.S., Rodin, I.A., Ikhalainen, Yu.A., Studenikin, F.R., Chernyaev, A.P., Shinkarev, O.V. & Yurov, D.S. Determination of chemical and microbiological characteristics of meat products treated by radiation. Industrial laboratory. Diagnostics of materials. **87**, 5–13 https://doi.org/10.26896/1028-6861-2021-87-6-5-13 (2021).
15. Ntakatsane, M.P., Liu, X.M. & Zhou, P. Rapid detection of milk fat adulteration with vegetable oil by fluorescence spectroscopy. J. Dairy Sci. **96**, 2130–2136 https://doi.org/10.3168/jds.2012-6417 (2013).
16. Xie, P., Chen, S., Liang, Y.-Z., Wang, X., Tian, R. & Upton, R. Chromatographic fingerprint analysis—a rational approach for quality assessment of traditional Chinese herbal medicine. J. Chromatogr. A **1112**, 171–180 https://doi.org/10.1016/j.chroma.2005.12.091 (2006).
17. Zhu, Y., Wang, J., Wu, Y., Shang, Z., Ding, Y. & Hu, A. A fluorescent sensor array-based electronic tongue for Chinese tea discrimination. J. Mater. Chem. C, **9**, 5676–5681. DOI: 10.1039/d1tc00491c (2021).
18. Zil'berg, R.A., Yarkaeva, Yu.A., Maksyutova, E.I., Sidel'nikov, A.V. & Maistrenko, V.N. Voltammetric identification of insulin and its analogues using glassy carbon electrodes modified with polyarylenephthalides. J. Anal. Chem. **72**, 402–409 https://doi.org/10.1134/S1061934817040177 (2017).

19. Bajoub, A., Medina-Rodríguez, S., Gómez-Romero, M., Ajal, E.A., Bagur-González, M.G., Fernández-Gutiérrez, A. & Carrasco-Pancorbo, A. Assessing the varietal origin of extra virgin olive oil using liquid chromatography fingerprints of phenolic compound, data fusion and chemometrics. Food Chem. **215**, 245–255 https://doi.org/10.1016/j.foodchem.2016.07.140 (2017).
20. Novakowski, W., Bertotti, M. &, Paixão, T.R.L.C. Use of copper and gold electrodes as sensitive elements for fabrication of an electronic tongue: discrimination of wines and whiskies. Microchem. J. **99**, 145–151 https://doi.org/10.1016/j.microc.2011.04.012 (2011).
21. Andrade, J.M., Kubista, M., Carlosena, A. & Prada, D. 3-way characterization of soils by Procrustes rotation, matrix-augmented principal components analysis and parallel factor analysis. Anal. Chim. Acta **603**, 20–29 https://doi.org/10.1016/j.aca.2007.09.043 (2007).
22. Brunelle, E., Huynh, C., Le, A.M., Halámková, L., Agudelo, J. & Halámek, J. New horizons for ninhydrin: colorimetric determination of gender from fingerprints, Anal. Chem. **88**, 2413–2420 https://doi.org/10.1021/acs.analchem.5b04473 (2016).
23. Madhuri, S., Vengadesan, N., Aruna, P., Koteeswaran, D., Venkatesan, P. & Ganesan, S. Native fluorescence spectroscopy of blood plasma in the characterization of oral malignancy, Photochem. Photobiol. **78**, 197–204 https://doi.org/10.1562/0031-8655(2003)078<0197:nfsobp>2.0.co;2 (2003).
24. Sádecká, J. &; Tóthová, J. Fluorescence spectroscopy and chemometrics in the food classification—A review. *Czech J. Food Sci.*, **25**, 159–173 https://www.agriculturejournals.cz/publicFiles/00302.pdf (2007).
25. Karoui, R. & Blecker, C. Fluorescence spectroscopy measurement for quality assessment of food systems—A review. *Food Bioproc. Technol.*, **4**, 364–386 https://doi.org/10.1007/s11947-010-0370-0 (2011).
26. Han, J., Wang, B., Bender, M., Kushida, S., Seehafer, K. & Bunz, U.H.F. Poly(aryleneethynylene) Tongue Identifies Nonsteroidal Anti-inflammatory Drugs in Water: A Test Case for Combating Counterfeit Drugs, ACS Appl. Mater. Interf. **9**, 790–797 https://doi.org/10.1021/acsami.6b11690 (2017).
27. Sun, S., Jiang, K., Qian, S.,Wang, Y. & Lin, H. Applying Carbon Dots-Metal Ions Ensembles as a Multichannel Fluorescent Sensor Array: Detection and Discrimination of Phosphate Anions, Anal. Chem., **89**, 5542–5548 https://doi.org/10.1021/acs.analchem.7b00602 (2017).
28. Divyanin, N.N., Razina, A.V., Rukosueva, E.A., Garmash, A.V. & Beklemishev, M.K. Discrimination of 2-3-component mixtures of organic analytes by a “fluorescent tongue”, Microchem. J., **135**, 48–54 https://doi.org/10.1016/j.microc.2017.08.002 (2017).
29. Abdel-Ghany, M.F., Hussein, L.A., Ayad, M.F. & Youssef, M.M. Investigation of different spectrophotometric and chemometric methods for determination of entacapone, levodopa and carbidopa in ternary mixture, Spectrochim. Acta. A **171**, 236–245 https://doi.org/10.1021/acs.analchem.7b00602 (2017).
30. Rukosueva, E.A., Dobrolyubov, E.O., Goryacheva, I.Yu. & Beklemishev, M.K. Discrimination of whiskies using an “add-a-fluorophore” fluorescent fingerprinting strategy, Microchem. J. **145**, 397–405 https://doi.org/10.1016/j.microc.2018.11.002 (2019).

31. Gitlin, Yu., Surkova, A., Ivonina, M.V., Sizov, V.V., Petrovskii, S.K., Legin, A., Starova, G.L., Koshevoy, I.O., Grachova, E.V. & Kirsanov, D.O. Cyclometalated Ir(III) complexes as tuneable multiband light sources for optical multisensor systems: Feasibility study. Dyes. Pigm. **180**, 108428 https://doi.org/10.1016/j.dyepig.2020.108428 (2020).
32. Rukosueva, E.A., Belikova, V.A., Krylov, I.N., Orekhov, V.S., Skorobogatov, E.V., Garmash, A.V. & Beklemishev, M.K. Evaluation of Discrimination Performance in Case for Multiple Non-Discriminated Samples: Classification of Honeys by Fluorescent Fingerprinting. Sensors, **20**, 5351 https://doi.org/10.3390/s20185351 (2020).
33. Zakharenkova, S.A., Katkova, E.A., Doroshenko, I.A., Kriveleva, A.S., Lebedeva, A.N., Vidinchuk, T.A., Shik, A.V., Abramchuk, S.S., Podrugina, T.A. & Beklemishev, M.K. Aggregation-based fluorescence amplification strategy: "turn-on" sensing of aminoglycosides using near-IR carbocyanine dyes and pre-micellar surfactants. Spectr. Acta A, **247**, 119109. https://doi.org/10.1016/j.saa.2020.119109 (2021).
34. Doroshenko, I.A., Aminulla, K.G., Azev, V.N., Kulinich, T.M., Vasilichin, V.A., Shtil, A.A., & Podrugina, T.A. Synthesis of modified conformationally fixed tricarbocyanine dyes for conjugation with therapeutic agents. Mendeleev Commun., **31**, 615–617 https://doi.org/10.1016/j.mencom.2021.09.008 (2021).
35. Shik, A.V., Stepanova, I.A., Doroshenko, I.A., Podrugina, T.A. & Beklemishev, M.K. Carbocyanine-Based Fluorescent and Colorimetric Sensor Array for the Discrimination of Medicinal Compounds. Chemosensors, **10**, 88. https://doi.org/10.3390/chemosensors10020088 (2022).
36. Narayanan, N. & Patonay, G.A. New Method for the Synthesis of Heptamethine Cyanine Dyes: Synthesis of New Near-Infrared Fluorescent Labels. J. Org. Chem. **60**, 2391–2395. https://doi.org/10.1021/jo00113a018 (1995).
37. Chernyaev, A.P., Avdyukhina, V.M., Bliznyuk, U.A. *et al.* Bull. Russ. Acad. Sci. Physics. **84**, 385–390. https://doi.org/10.3103/S106287382004005X (2020).
38. Jolliffe, I. Principal Component Analysis. 2nd ed, Springer, 2002.
39. Stepanova, I.A., Lebedeva, A.N., Shik, A.V., Skorobogatov, E.V. & Beklemishev, M.K. Recognition and Determination of Sulfonamides by Near-IR Fluorimetry Using Their Effect on the Rate of the Catalytic Oxidation of a Carbocyanine Dye by Hydrogen Peroxide. J. Analyt. Chem. **76**, 1397–1405. https://doi.org/10.1134/S1061934821120121 (2021).
40. Kozuch, D.J., Ristroph, K., Prud'homme, R.K. & Debenedetti, P.G. Insights into Hydrophobic Ion Pairing from Molecular Simulation and Experiment. ACS Nano **14**, 6097–6106. https://doi.org/10.1021/acsnano.0c01835 (2020).

Figures

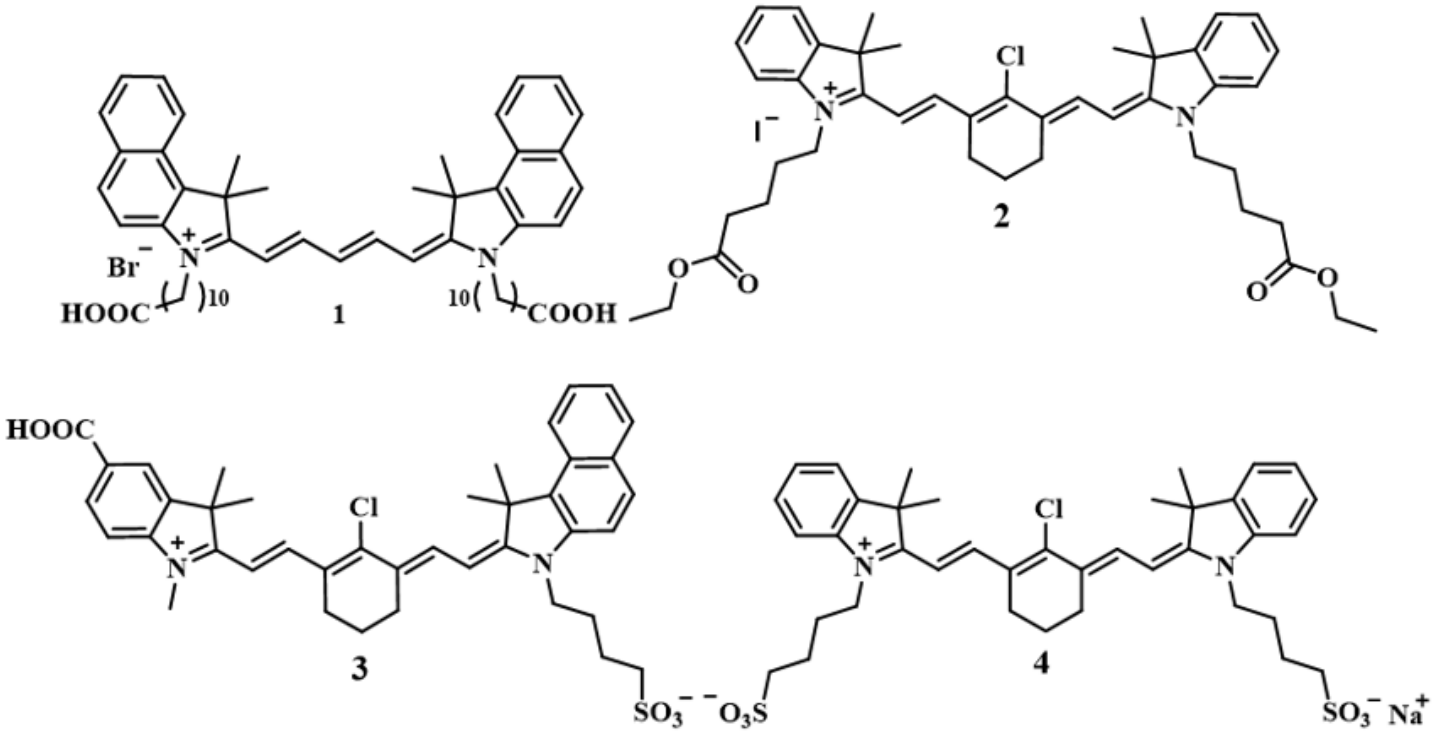

Figure 1

Structures of the dyes used in optical “fingerprinting” of potatoes.

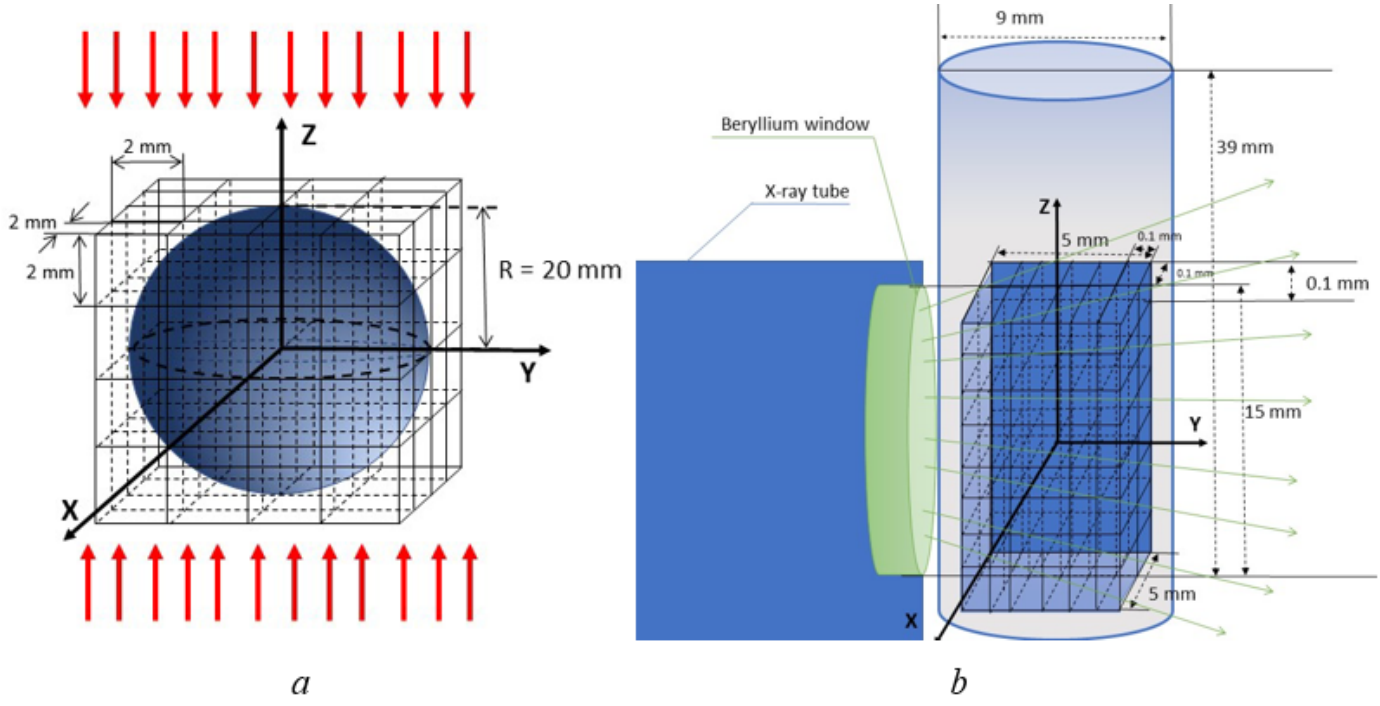

Figure 2

Modelling the two-side irradiation of a potato tuber: *a* – with 1 MeV electrons, *b* – with X-rays.

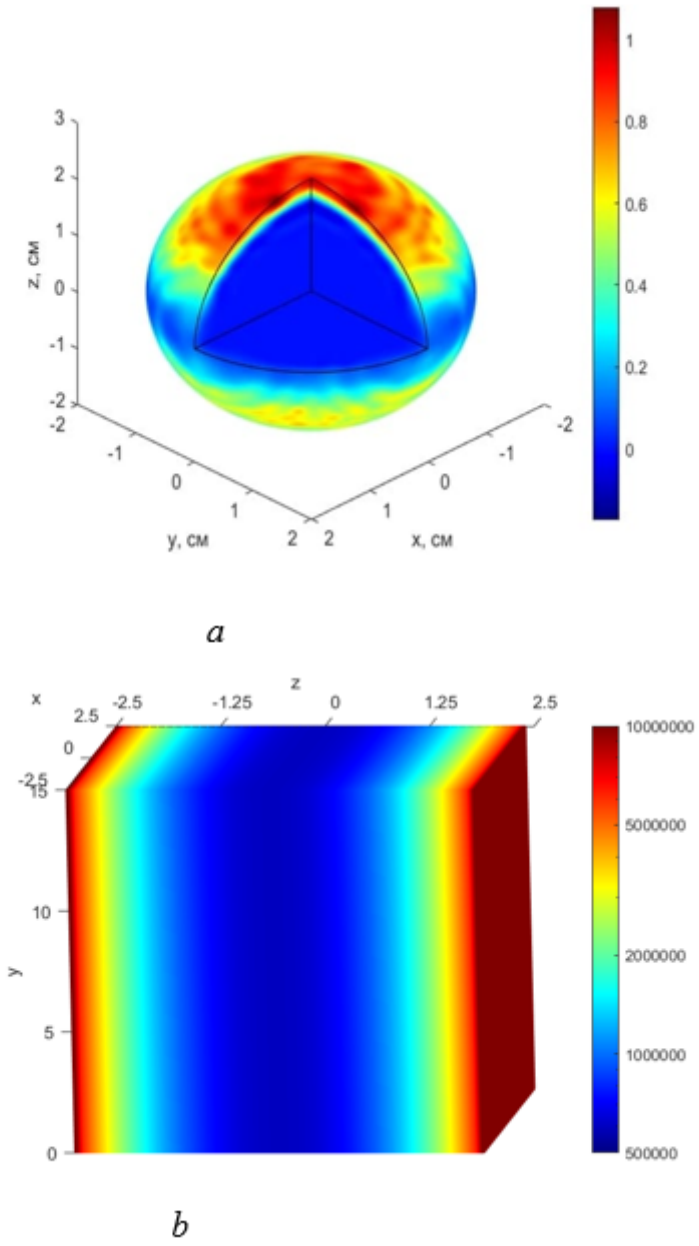

Figure 3

Relative dose distribution in the Φ 4 cm water sphere (a) and 6 mm thick, 6 mm long and 15 mm high water parallelepiped (b).

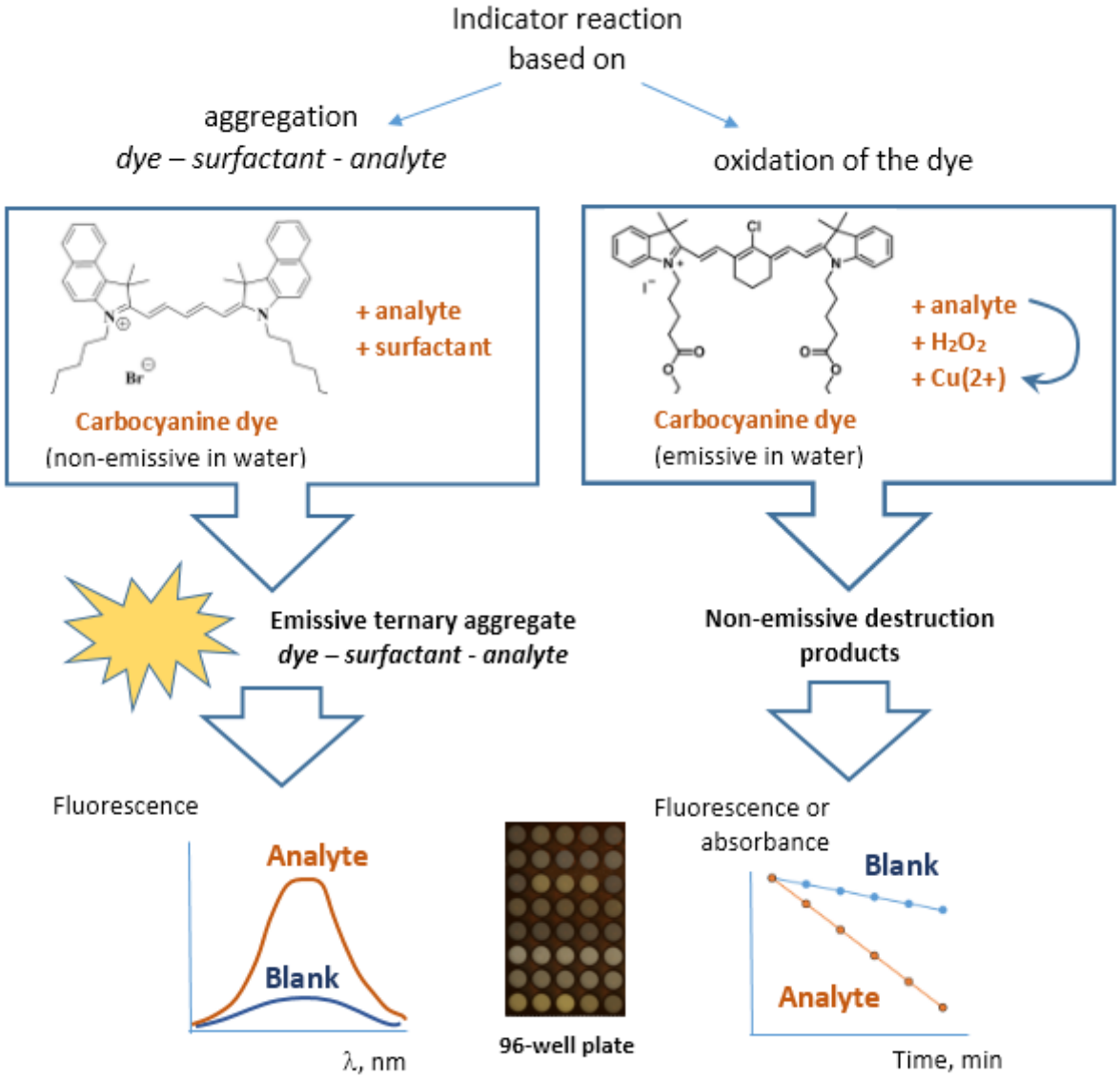

Figure 4

Principles underlying indicator reactions used in sensing. Analyte is an unknown compound formed as a result of radiation interaction with the sample.

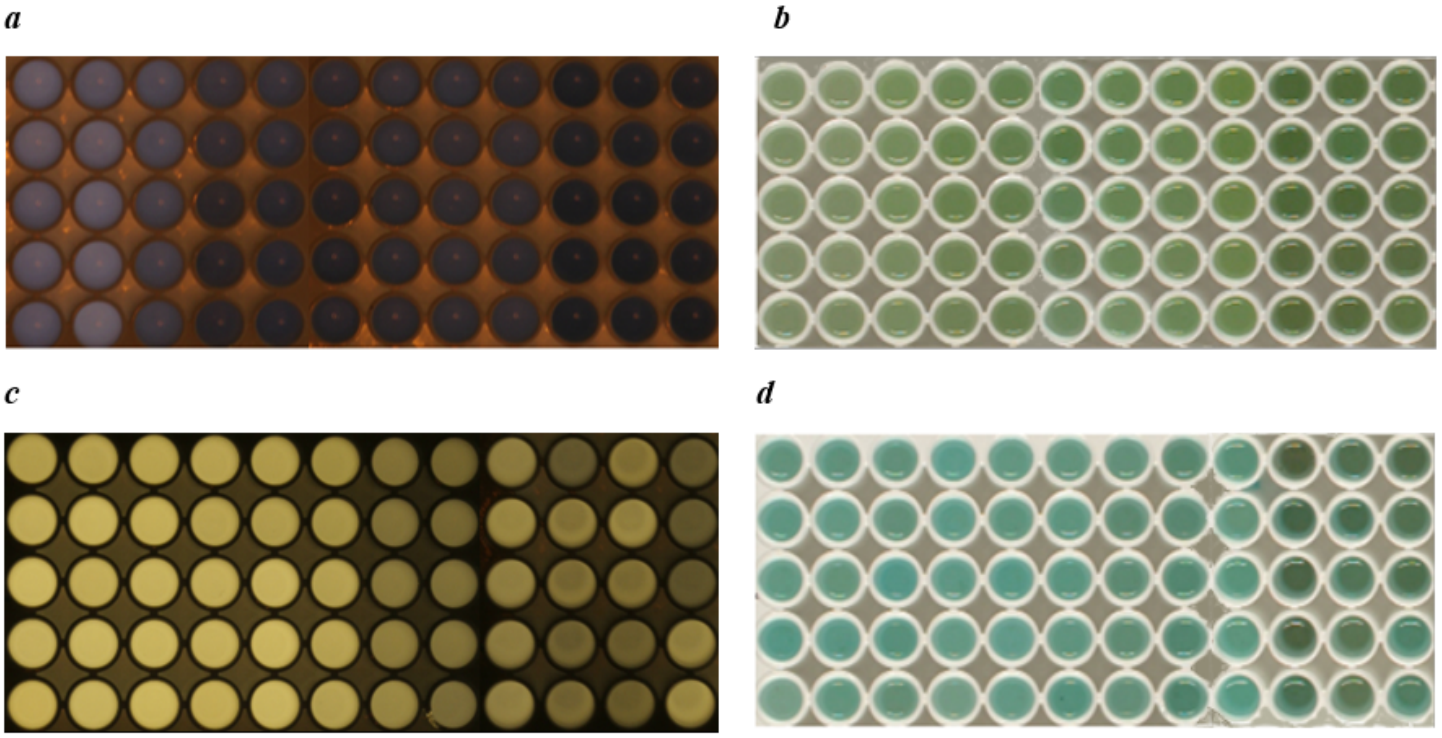

Figure 5

Examples of photographs of the plates for the redox indicator reaction (oxidation of dye **2** with hydrogen peroxide: *a* and *b*) and the aggregation-type indicator reaction (with dye **1**: *c* and *d*) in the NIR region (*a, c*) and visible light (*b*, *d*). Three different tubers were studied for each radiation dose; an aqueous extract of a sample of one tuber (extracted with the addition of ascorbic acid) was placed into each of the five wells arranged in vertical rows. Sample order, left to right: columns 1–3: 0 Gy (non-irradiated); 4–6: 100 Gy; 7–9: 1 kGy; columns 10–12: 10 kGy. The time from the start of the redox reaction (*a, b*) was 11 min, the photographs for the aggregation-type reaction (*b, c*) were taken immediately after mixing the solutions.

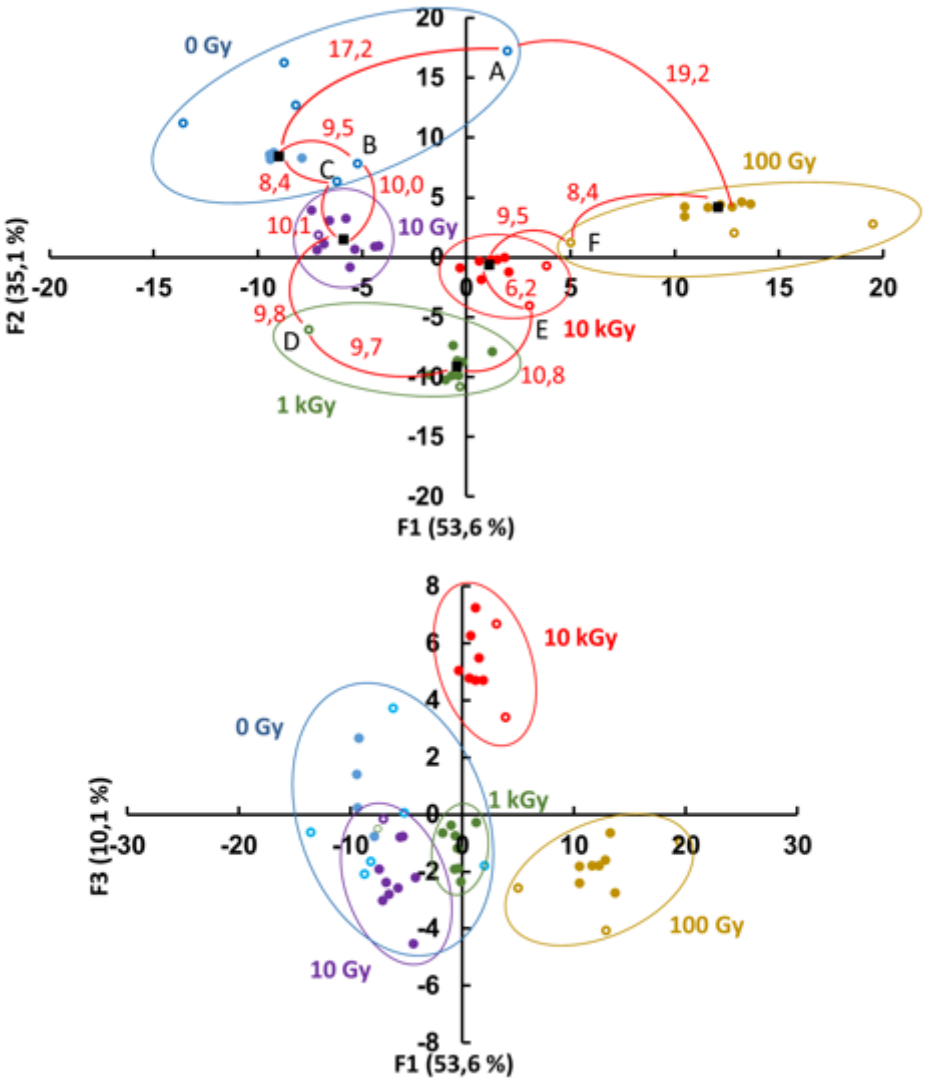

Figure 6

Discriminant analysis score plots for experiment No 1 performed with potatoes of the same variety irradiated with electron beam (doses from 10 Gy to 10 kGy) and a control (0 Gy), two tubers for each dose. Coordinates: *a* – F1–F2, *b* – F1–F3; 20 columns of data, based on three indicator reactions, were used for constructing the graphs (see Supplementary Table S2). Filled signs are training points, and empty signs are validation points.

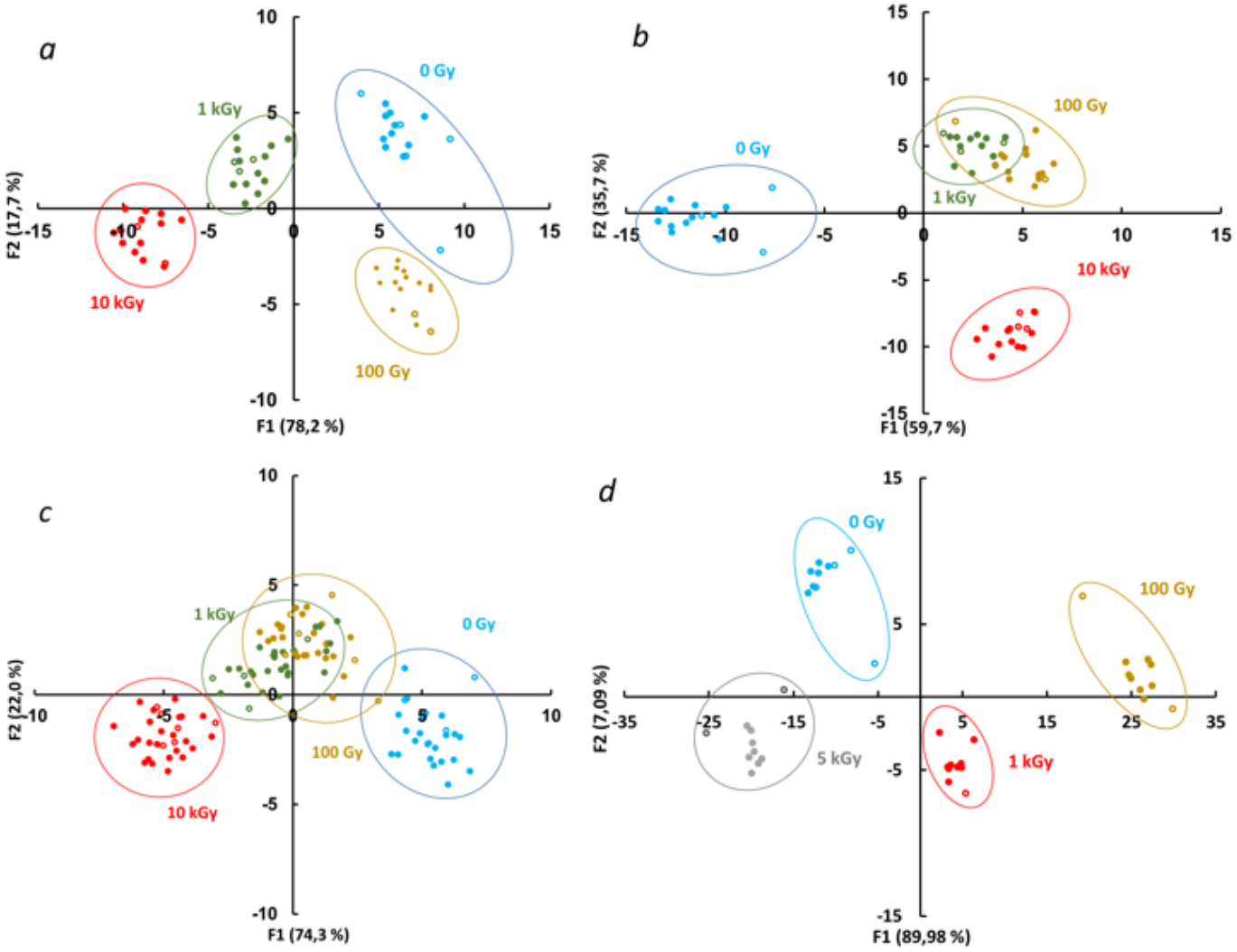

Figure 7

Discriminant analysis score plots for experiment No 2 (electron beam irradiation, *a*–*c*) and X-ray irradiation (*d*). Irradiation with electron beam was performed for potatoes of variety X (*a*), variety Y (*b*), and two mixed varieties (X and Y) (*c*) with doses 0 (control), 100 Gy, 1 and 10 kGy, 3 tubers with each dose. Irradiation with X-rays was performed with doses 0, 100 Gy, 1 and 5 kGy, 2 tubers for each dose. Validation points (total amount of 12 for *a* and *b*, 25 for *c*, 8 for *d*) are shown as empty signs, and training points as full signs. Only one validation run is exemplified in each graph.

Supplementary Files

This is a list of supplementary files associated with this preprint. Click to download.

- SupplementaryinformationShik.pdf